

Hot-Spot Mix in Direct-Drive DT Cryogenic Implosions:

Hydrodynamic mixing of ablator material into the hot spot of a direct-drive DT cryogenic implosion was diagnosed on OMEGA using an x-ray spectroscopy technique developed at the National Ignition Facility for x-ray-driven, ignition-scale implosions.^{1–3} The hot-spot mix mass enhances the radiative cooling of the hot spot and may cause a detrimental reduction in the hot-spot temperature and the neutron yield.^{4,5} The 8- μm -thick plastic (CH) ablator surrounding the 50- μm -thick DT ice layer was uniformly doped with trace amounts (0.4 to 0.7 at. %) of Ge as shown in Fig. 1(a). The Ge dopant in the plastic ablator is used to track the hydrodynamic mixing of the ablator material through the compressed DT shell and into the hot spot around stagnation as illustrated in Fig. 1(b). During the acceleration phase, the ablation-front Rayleigh–Taylor hydrodynamic instability—seeded by laser imprint,⁶ target-surface debris, and the mounting stalk—mixes ablator material into the DT vapor region of the target.^{1–3,7} These short-wavelength perturbations are predicted to limit the performance of low-adiabat implosions ($\alpha < 3$) (Ref. 7). A systematic study of hot-spot mix on the implosion adiabat was conducted for the following calculated adiabat values: $\alpha = 2.5, 4,$ and 7 . Future Ge-doped ablator designs will investigate the stability of the ablator/DT ice interface, since radiation preheat can influence the Atwood number at this interface.

The experimental signature of hot-spot mix—the Ge K-shell and satellite emission—was recorded using time-integrated x-ray spectrometers having a spectral resolving power of 2000 and a 1-D imaging spatial resolution of either 40 μm or 150 μm . If the Ge reaches the hot spot, it will emit the signature emission. The spatial resolution was sufficient to resolve the hot-spot emission from the rest of the implosion. The measured Ge K-shell and satellite emission from the hot spot was analyzed with an atomic physics code assuming uniform space and time plasma conditions to diagnose the hot-spot mix mass.^{2,3} The brightness of the Ge K-shell emission depends on the electron density (n_e), electron temperature (T_e), and the areal density of Ge (ρR_{Ge}). The measured spectrum along with the best and 1σ fits and the inferred mix mass quantities are presented in Fig. 2 for the $\alpha = 2.5$ implosion, which has an inferred mix mass in the 1- to 5-ng range. Similar spectra were recorded and analyzed for the higher-adiabat implosions. Preliminary analysis shows the hot-spot mix mass is below 50 ng and decreases slightly as the calculated adiabat is increased. As shown in Fig. 3 for the $\alpha = 2.5$ implosions, a lower neutron yield is measured with a higher amount of inferred hot-spot mix mass. The objective of the next round of experiments is to identify the short-wavelength seeds of the hot-spot mix mass.

Omega Facility Operations Summary: The Omega Laser Facility conducted 168 target shots in October with an average experimental effectiveness (EE) of 87.2% (124 shots on OMEGA with an EE of 84.7% and 44 on OMEGA EP with an EE of 94.3%). The ICF program accounted for 67 target shots, all taken by LLE-led teams. Eighty-one shots were taken for the HED program by LANL, LLE, LLNL, and SNL teams. A Princeton-led NLUF team conducted 8 target shots and 12 shots were taken for a CELIA (France)-led experiment.

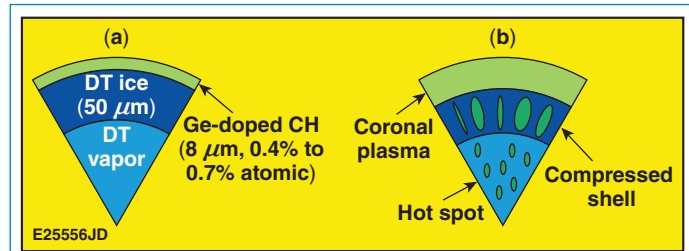


Figure 1. Schematic of (a) the direct-drive layered DT cryogenic target with a Ge-doped plastic ablator and (b) the hydrodynamic mixing of the ablator material into the compressed shell and hot spot around stagnation.

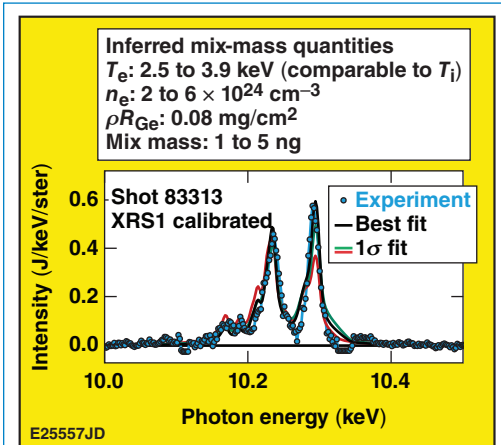


Figure 2. The measured spatially integrated and time-integrated Ge K shell and satellite emission from the hot spot is fitted with an atomic physics code to infer the mix mass quantities for the $\alpha = 2.5$ implosion.

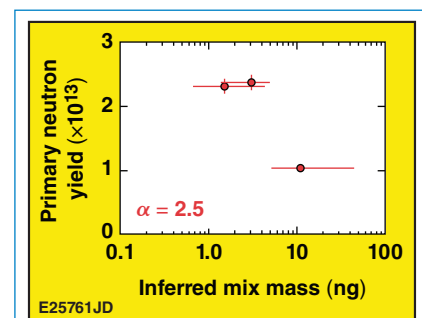


Figure 3. The measured primary neutron yield versus the inferred mix mass.

1. B. A. Hammel *et al.*, Phys. Plasmas **18**, 056310 (2011); 2. S. P. Regan *et al.*, Phys. Plasmas **19**, 056307 (2012); 3. S. P. Regan *et al.*, Phys. Rev. Lett. **111**, 045001 (2013); 4. T. Ma *et al.*, Phys. Rev. Lett. **111**, 085004 (2013); 5. T. C. Sangster *et al.*, Phys. Plasmas **20**, 056317 (2013); R. Epstein *et al.*, Phys. Plasmas **22**, 022707 (2015); 6. S. X. Hu *et al.*, Phys. Plasmas **17**, 102706 (2010); 7. I. V. Igumenshchev *et al.*, Phys. Plasmas **20**, 082703 (2013).